# Development of a Black Start Decision Supporting System for Isolated Power Systems

Yi-Ting Chou, Chih-Wen Liu, *Fellow, IEEE*, Yi-Jen Wang, Chin-Chung Wu, and Chao-Chi Lin

***Abstract*—Black start is the primary procedure deployed for rapid recovery from a complete blackout. For isolated power systems such as the Taiwan power system (TPS), a reliable and efficient black start procedure is more important than interconnected power systems. In this paper, a black start decision-supporting system (BSS) with an interactive graphical user interface (GUI) has been developed. BSS can rapidly generate optimal black start strategies according to the updated system data configuration and objective function; furthermore, BSS can automatically simulate the strategies and visualize the results. By applying the BSS to evaluate the black start strategies for TPS, the effectiveness of BSS has been demonstrated. The BSS has been utilized by Taiwan Power Company (TPC) for black start planning with comparison to traditional manual planning. With the aid of BSS, the dispatchers are equipped with more support and the restoration risk can be much alleviated.**

***Index Terms*—Black start, decision support system, graphical user interfaces (GUI), power systems.**

## I. Introduction

NOWADAYS, the demand for reliable and sufficient power supply is becoming increasingly intensive. Although the reliability of power supply has been enhanced by progressive controlling apparatus, there is still a possibility of large area blackout, such as the Northeast Blackout of 2003 in the United States and Canada [1] and the blackout in Japan on March 11th, 2011 caused by the tsunami [2]. Since Taiwan is located on the Pacific Ocean seismic zone and the subtropical monsoon climate region, power system infrastructures risk being damaged by earthquakes, landslides, typhoons, and mudflows. Also, the increased load has caused decreased stability in TPS and raised the possibility of blackouts. As an isolated power network with a confined structure due to the land shape, TPS is likely to collapse if a fault is not handled properly due to the failure or mal-operation of protection devices. Since 1976, Taiwan has suffered over two large-scale blackouts [3], [4], which have caused considerable economic loss and threatened national security. To facilitate the service recovery and reduce the relating loss, black start, the procedure to restore power supply by self-starting black start units (BSU), is the first task after a severe blackout occurs.

Due to the complex characteristics of the power systems under an extreme condition, black start is commonly formulated as a multi-objective and dynamic decision-making problem. Various problems and issues related to generators, power devices and transmission systems have been carefully studied for the improvement in power restoration [5]–[10]. Based on the general restoration guidelines [11]–[15] and the experience of operators, power utilities used to pre-establish the black start schemes to meet their particular criteria and requirements. However, due to unexpected situations, black start is rarely progressed exactly as planned. To automatically generate the most suitable black start schemes, knowledge-based expert systems functionally strengthened by the decision supporting techniques have been widely utilized [16]–[20]. Emerging modern optimization techniques have also received much attention to solve the multi-objective problems [21]–[23].

As the state-of-the-art publications in regards to black start decision making mostly focus on the approaches and algorithms [24]–[28] yet putting less illustration on the tool realization for actual power systems, this paper presents not only the formulation and optimization methodology to the black start problem that comprises multiple factors regarding system characteristics, components, and simulation results, but also the structure, tasking and linking of the core modules of the developed decision-supporting tool named BSS for actual isolated power systems such as TPS. Since the problem is a non-differentiable mixed integer nonlinear programming (MINLP) problem that is difficult to be solved by traditional mathematical optimization techniques, a hybrid approach combining the graph algorithm and swarm intelligence is adopted to achieve the optimal solutions. With the modular structure and multi-thread programming, the developed BSS can efficiently evaluate the optimal black start strategies according to the prevailing system condition and the planning objectives. Moreover, the BSS can ease the verification process by the function of simulation automation. Through practical application to TPS, it is justified that the BSS is able to compute the optimal black start strategies in a timely fashion, including the ones established manually by TPC dispatchers and also the alternative plans which are not explored by the manual planning, in sense of minimizing the value of the formulated objective function [29].

The paper is organized as follows: Section II describes the formulation of the black start optimization problem. Section III delineates the optimization algorithm and the composing modules of BSS. Section IV demonstrates the applicability and

Manuscript received January 08, 2012; revised February 08, 2012; accepted December 15, 2012. Date of publication January 24, 2013; date of current version July 18, 2013. This work was supported in part by Taiwan Power Company under Contract TPC-546-2101-9501 and the National Science Council under Contract NSC 100-3113-P-002-012. Paper no. TPWRS-00025-2012.

Y.-T. Chou and C.-W. Liu are with the Department of Electrical Engineering, National Taiwan University, Taipei 106, Taiwan, R.O.C (e-mail: d97921012@ntu.edu.tw; cwliu@cc.ee.ntu.edu.tw).

Y.-J. Wang is with the Graduate Institute of Electrical Engineering Department, Tungnan University, New Taipei City 222, Taiwan (e-mail: yjwang@mail.tnu.edu.tw).

C.-C. Wu and C.-C. Lin are with the Department of System Operations, Taiwan Power Company, Taipei City 100, Taiwan (e-mail: u026955@taipower.com.tw; u850899@taipower.com.tw).

Color versions of one or more of the figures in this paper are available online at http://ieeexplore.ieee.org.

Digital Object Identifier 10.1109/TPWRS.2013.2237792

adaptability of BSS. Finally, the conclusion is presented in Section V.

## II. Problem Formulation

The formulation of the black start optimization problem is the fundamental base to develop the most important computation module of BSS. In this section, the problem formulation, including the objective function and constraints, is illustrated in detail.

### A. Objective Function

For the ease of illustration of the proposed objective function, we first define $\mathbf{R}$ as the matrix representing a black start path in the transmission system with $M$ buses by

$$\mathbf{R} = [r_{ij}]_{M\times M} \tag{1}$$

where $r_{ij} = 1$ if the $i^{\text{th}}$ energizing bus (i.e., the energizing bus in the $i^{\text{th}}$ order) in the black start path is Bus $j$, otherwise $r_{ij} = 0$. Since the repeated energization is not allowed and the total number of the energized buses along the black start path is one more than the number of switches to be operated, the two relations among the entries $r_{ij}$ are derived as

$$\sum_{j=1}^{M} r_{ij} \in \{0,1\} \quad \forall i \in \{0,1,2,\ldots,M\} \tag{2}$$

$$\sum_{i=1}^{M}\sum_{j=1}^{M} r_{ij} = N+1 \tag{3}$$

where $N$ denotes the number of switches to be operated in the energizing path.

The overall objective of black start is to apply voltage from the BSUs to the target units through the transmission system as quickly and safely as possible; thus, the objective function is to seek the $\mathbf{R}$ which has the lowest cost in terms of the efficiency and security of the energizing procedure. In this study, the cost is expressed as a function of $\mathbf{R}$, namely, $C(\mathbf{R})$, which encompasses two sub cost functions: the cost related to the efficiency of the BSUs and target units, i.e., $C_{\text{U}}(\mathbf{R})$, and the cost related to the efficiency and security of the power transmission process, i.e., $C_{\text{P}}(\mathbf{R})$. The items in the two sub functions are normalized with respect to their corresponding optimums. The detailed illustration of $C_{\text{U}}(\mathbf{R})$ and $C_{\text{P}}(\mathbf{R})$ are as follows.

*1) $C_{\text{U}}(\mathbf{R})$, Cost Related to the Units:* Based on engineering judgment, we formulate $C_{\text{U}}(\mathbf{R})$ by the efficiency indices of the participating BSU and target unit, respectively, in the given $\mathbf{R}$. The efficiency index of a unit is defined by the unit's startup time, generation capacity, and the total relative switching times to the other units, which are all very important factors to affect the efficiency of restoration and the service recovery. As seen in

$$\alpha = \frac{1}{D_B}\cdot\left(\frac{P_b}{T_B}\right), \qquad \text{where} \quad D_B = \sum_{i=1}^{K_t} a_i. \tag{4}$$

$$\beta = \frac{1}{D_T}\cdot\left(\frac{P_g - P_c}{T_T}\right), \qquad \text{where} \quad D_T = \sum_{j=1}^{K_b} b_j \tag{5}$$

the efficiency indices of a BSU and a target unit are defined as $\alpha$ and $\beta$, respectively, and where

- $P_b$ capacity of the BSU;
- $T_B$ startup time of the BSU;
- $T_T$ startup time of the target unit;
- $P_g$ maximum power generation of the target unit;
- $P_c$ consuming power of the target unit;
- $K_t$ maximum number of targets, which is determined by (6);
- $K_b$ total number of BSUs;
- $a_i$ minimum required switching times to the $i$th target unit;
- $b_j$ minimum required switching times to the $j$th BSU.

The efficiency index of a unit can represent its priority during black start. The larger index corresponds to the higher priority. The number of $K_t$ can be determined by

$$\sum_{i=1}^{K_t} P_c^i \le \sum_{j=1}^{K_b} C_j \tag{6}$$

depending on the total capacity of the BSUs in the system, where $C_j$ denotes the capacity of the $j^{\text{th}}$ BSU, and $P_c^i$ stands for the consuming power $P_c$ of the target unit with the $i^{\text{th}}$ highest efficiency index. Note that the consuming power of the LNG units should be bundled with the power requirement of the corresponding LNG stations.

Having $\alpha$ and $\beta$, now we can formulate $C_{\text{U}}(\mathbf{R})$ as

$$C_U(\mathbf{R}) = \hat{U}_s + \omega_U \hat{U}_t^{\rho_U} \tag{7}$$

by the reverse of the normalized efficiency indices of the BSU and target unit, where $\hat{U}_s$ and $\hat{U}_t$ with the weight and penalty parameters, $\omega_U$ and $\rho_U$ are given by

$$\hat{U}_s = \frac{\alpha_0}{\alpha}$$

$$\hat{U}_t = \frac{\beta_0}{\beta}$$

where $\alpha_0$ and $\beta_0$ are the largest efficiency indices of BSU and target unit, respectively, among all of the BSUs and target units in the system.

*2) $C_{\text{P}}(\mathbf{R})$, Cost Related to the Power Transmission Risks:* $C_{\text{P}}(\mathbf{R})$ is composed of two parts: $F(\mathbf{R})$ and $S(\mathbf{R})$, which correspond to the cost associated to the system components and the cost reflected from the simulation result.

Considering the general guidelines [13]–[15], [30], [35] and based on engineering judgment [29], [31]–[34], $F(\mathbf{R})$ can be expressed by the three key factors which will highly affect the security and efficiency of the power transmission process. The three factors are illustrated as follows.

*The sum of susceptance*: While energizing transmission lines under light load condition, the accumulated susceptance of transmission line will cause overvoltage due to Ferranti effect and other transient behaviors, which would not only increase the failure rate of equipments such as transformers and breakers, but also lead to miss-tripping of protection relays that may fail black start operation.

*The number of switches*: The risk of harmful switching surges and other transient phenomenon would be increased with the

growing number of switches to be operated. Though many protection devices have been used to mitigate switching surges hazards, the action of these protection devices often produce relay tripping, which may fail the black start procedure. Also, as each switch operation needs to be under deliberate confirmation, the black start procedure will be prolonged when there are more switching operations in a black start path.

*The number of transformers*: While energizing the transmission grid during black start, the nonlinear behavior of transformers may cause potentially sustained non-harmonic oscillation and transient ferro-resonance overvoltage which would bring severe damage on transmission equipment. The large inrush current also increases miss-tripping possibility of the associated protection relays and the harmful impacts on transformers. For reducing the failure rates, the operation times of transformers during re-energization is also an important factor to be optimized.

Summing the above, $F(\mathbf{R})$ is expressed as

$$F(\mathbf{R}) = \omega_B \hat{B}^{\rho_B} + \omega_N \hat{N}^{\rho_N} + \omega_T \hat{T}^{\rho_T} \tag{8}$$

comprising the factors $\hat{B}$, $\hat{N}$, and $\hat{T}$ namely, the normalized sum of susceptance, number of switches, and number of transformers to be operated along the energizing path, respectively, where

$$\hat{B} = \frac{\sum_{i=1}^{N} B_i}{B_0}$$
$$\hat{N} = \frac{N}{N_0}$$
$$\hat{T} = \frac{T}{T_0}$$

where $B_i$ is the susceptance of the $i$th transmission line taking into account the equivalent susceptance of the available compensation devices, $N$ is the number of switches between the starting transmission bus and the terminal transmission bus, and $T$ is the number of total transformers in $\mathbf{R}$. $B_0$, $N_0$, and $T_0$ denote the minimal sum of susceptance excluding compensation devices, the minimal $N$, and the minimal $T$, respectively, among all of the possible energizing paths considering all the combination of end units.

On the other hand, $S(\mathbf{R})$ is formulated by the worst case simulation results of $\mathbf{R}$ since the simulation results can precisely demonstrate the influence of transmission constants on voltage variation at each bus and reflect the safety level. By making use of the root mean square (RMS) values, $\hat{V}_t$ and $\hat{V}_s$ of the simulated transient peak and steady-state voltages, respectively, at $N+1$ buses, $S(\mathbf{R})$ is expressed as

$$S(\mathbf{R}) = \omega_t \hat{V}_t^{\rho_t} + \omega_s \hat{V}_s^{\rho_s} \tag{9}$$

where

$$\hat{V}_t = \left( \frac{\|\mathbf{V_t}\|^2}{N+1} \right)^{0.5}$$
$$\hat{V}_s = \left( \frac{\|\mathbf{V_s}\|^2}{N+1} \right)^{0.5}$$

where $\mathbf{V_t}$ and $\mathbf{V_s}$ are the vectors composed of the sampled transient peak voltage $V_t^k$ (p.u.) and steady-state voltage $V_s^k$ (p.u.) at the $k$th energizing bus, as given, respectively, in

$$\mathbf{V_t} = [\, V_t^1 \quad V_t^2 \quad \cdots \quad V_t^k \quad \cdots \quad V_t^N \quad V_t^{N+1} \,]^{\mathrm{T}} \tag{10}$$
$$\mathbf{V_s} = [\, V_s^1 \quad V_s^2 \quad \cdots \quad V_s^k \quad \cdots \quad V_s^N \quad V_s^{N+1} \,]^{\mathrm{T}}. \tag{11}$$

Integrating $F(\mathbf{R})$ and $S(\mathbf{R})$, $C_{\mathrm{P}}(\mathbf{R})$ is further expressed as

$$C_{\mathrm{P}}(\mathbf{R}) = \hat{B} + \omega_1 \hat{N}^{\rho_1} + \omega_2 \hat{T}^{\rho_2} + \omega_3 \hat{V}_t^{\rho_3} + \omega_4 \hat{V}_s^{\rho_4} \tag{12}$$

where $\omega_1 = \omega_N/\omega_B$, $\omega_2 = \omega_T/\omega_B$, $\omega_3 = \omega_t/\omega_B$, and $\omega_4 = \omega_s/\omega_B$.

Finally, combining $C_{\mathrm{P}}(\mathbf{R})$ and $C_{\mathrm{U}}(\mathbf{R})$, the overall objective function is formulated as shown in

$$minimize\ C(\mathbf{R}) = C_{\mathrm{P}}(\mathbf{R}) + \omega \cdot C_U(\mathbf{R}). \tag{13}$$

Note that, if the starting BSU and target unit are specified, the objective function can be reduced to the minimization of $C_{\mathrm{P}}(\mathbf{R})$ with the localized values of $B_0$, $N_0$, and $T_0$.

### B. Constraints

The optimization problem is subject to the following general constraints [30], [35].

1) The limit of BSU's capacity is given by

$$P_b \geq P_c \tag{14}$$
$$P_{\min} \leq P_b \leq P_{\max} \tag{15}$$

where $P_{\min}$ to $P_{\max}$ are the lower and upper bounds of the BSU's capacity.

2) The boundaries of voltage secure range are given by

$$\|\mathbf{V_t}\|_\infty \leq \hat{V}_{\max} \tag{16}$$
$$\bar{V}_{\min} \leq V_s^k \leq \bar{V}_{\max} \tag{17}$$

where $\hat{V}_{\max}$ is the maximum overvoltage tolerance, while $\bar{V}_{\min}$ and $\bar{V}_{\max}$ are the lower and upper bounds of voltage secure range, respectively.

3) The limit of transmission lines' loading capacity is given by

$$P^k \leq P_{\max}^k \tag{18}$$
$$Q^k \leq Q_{\max}^k \tag{19}$$

where $P^k$ and $Q^k$ denote the real and reactive power of the $k$th energizing transmission line with the maximum loading capacity of $P_{\max}^k$ and $Q_{\max}^k$, respectively.

## III. Methodology and Structure of BSS

### A. Optimization Approach

The optimization problem of (13) is a MINLP. As a graph search problem, it is also a NP-complete problem since the searching graph contains negative cycles due to the negative susceptance values. It is rather difficult, if not impossible, to solve problems of such kind using mathematical programming techniques. Thus, we resort to a hybrid optimization approach combining a path tracing algorithm based on the property of

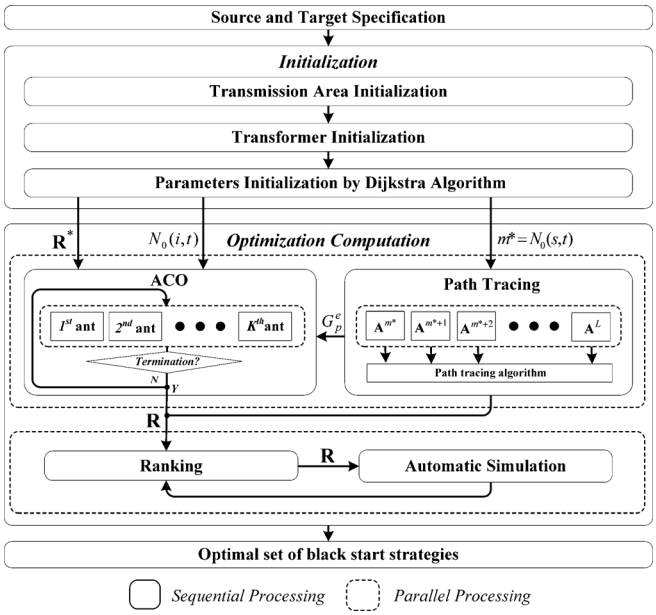


Fig. 1. Optimization methodology of BSS.

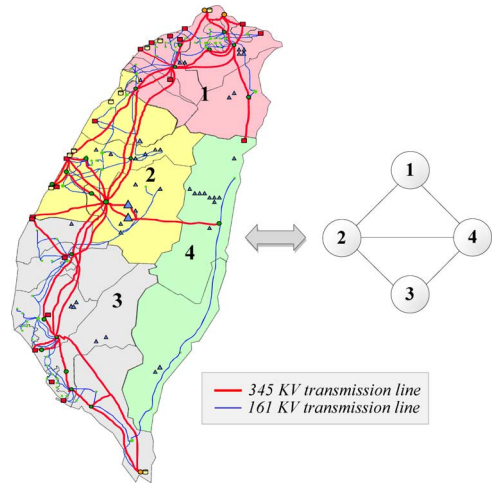


Fig. 2. Adjacency graph of the transmission regions in TPS.

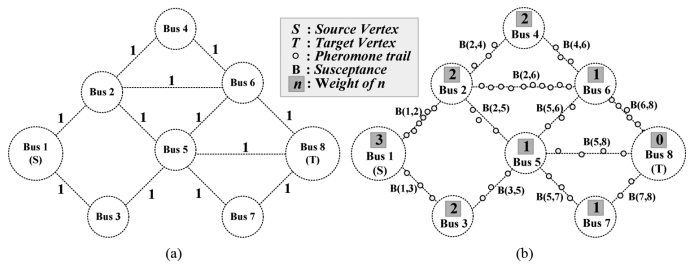


Fig. 3. (a) Adjacency graph. (b) Construction graph.

adjacency matrix and an Ant Colony Optimization (ACO) algorithm that holds the merits including: the distributed computation structure to be easily multi-threaded, the flexibility to be embedded with alternative algorithms for state transition and parameters update, and the adaptability to the system change. The methodology is depicted in Fig. 1, including the initialization and optimization computation phases. The two phases are described in the sequel.

*1) Initialization Phase:*

*Step 1: Searching scope initialization*

Regarding each transmission region as a node as shown in Fig. 2, one can derive a regional adjacency matrix ($\mathbf{Y}$). Suppose the BSU and the target unit locate at Node $i$ (Region $i$) and Node $j$ (Region $j$), respectively, and the entry in row $i$ and column $j$ of the $\mathbf{Y}$ raised to the $d_{\max}^{\text{th}}$ power is more than or equal to 1, i.e., $\mathbf{Y}_{i,j}^{d_{\max}} \geq 1$. Only the nodes on the paths passing through $d+1$ regions (for $d = d_{\min}$ to $d_{\max}$) from Region $i$ to Region $j$ are included in the valid searching scope. $d_{\max}$ is the upper boundary of $d$ referring to the utility's planning requirement (e.g., for TPC, $d_{\max}$ is set to 1) and $d_{\min}$ is the minimal $d$ such that $\mathbf{Y}_{i,j}^{d} \geq 1$.

*Step 2: Transformer state initialization*

The default statuses of transformers are configured as switched off except for those connecting the end units to the transmission system. If the end transmission buses are of different voltage levels, the statuses of the essential step-up or step-down transformers closely around the end transmission buses will be reconfigured as switched on. This step is necessary when the transmission voltage is required to be kept in the same level as far as possible during black start, such as addressed in TPC's black start planning criteria [29], [31].

*Step 3: Parameters initialization*

With the adjacency graph of transmission system as illustrated in the symbolical Fig. 3(a), where the vertices represent the buses and the edges with equal weight of 1 represent the branch lines, one can derive the minimum number of passing edges/switches, i.e., $m^*$ (also equals $N_0(s,t)$), and the paths $\mathbf{R}^*$ of minimum edges/switches among all the possible paths from the source vertex $v_s$ to the target vertex $v_t$ by Dijkstra algorithm. The minimal number of passing edges/switches from each vertex $v_i$ to the target vertex $v_t$, i.e., $N_0(i,t)$, will also be computed by Dijkstra algorithm and be used to represent the weight of each vertex, as the number marked upon each vertex in Fig. 3(b). These parameters will be utilized in the following phase.

*2) Optimization Computation Phases:* In this phase, we combine the path search principle of ACO [36] and the property of adjacency matrix based on Graph Theory to yield optimal black start paths. By giving favor to the candidates of high potential, the optimization procedure can be accelerated while maintaining the foraging diversity in the stochastic process. Since the minimization of transformers' operation times as the highest priority [29], [31] has been ensured by Step 2, the optimization can now be focused on the remaining factors. In ACO, as the switching operation relates to the risk of high surges and the prolonged restoration procedure [32], the favor would be distributed to the candidates of fewer passing switches [29], [31], which in a sense serve as a promising solution base from which the intelligent swarm's moves would diverge and auto-catalyze. The four procedures in this phase are described as follows.

*Procedure 1: Ant colony system initialization*

A weighted construction graph $G_a$ $(V, E, P)$ is first established as depicted in the symbolical Fig. 3(b), where $V$ is the set of vertices weighing $N_0(i,t)$, $E$ is the set of susceptance-weighted edges that fully connect all the vertices, and $P$ is a vector whose components represent the pheromone trail

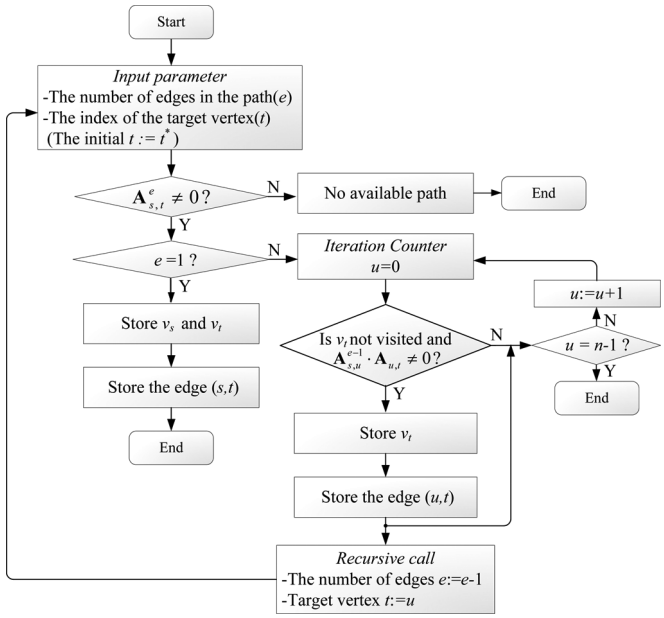


Fig. 4. Flowchart of the path tracing algorithm based on the property of adjacency matrix.

strength. The pheromone trail strength $\tau(i,j)$ on the edge $(i,j)$ that connects $v_i$ and $v_j$ is initialized by

$$\tau(i,j) = \begin{cases} \omega_1 \cdot \mu(i,j), & (i,j) \in E(\mathbf{R}^*) \\ \mu(i,j), & \text{otherwise} \end{cases} \tag{20}$$

where $\mu(i,j)$ is a small positive value and $E(\mathbf{R}^*)$ is the set of edges composing the path $\mathbf{R}^*$. $K$ ants are initially positioned on the starting vertex that represents the connecting transmission bus of BSU.

*Procedure 2: Solution construction*

Each ant will move randomly to construct its solution by incrementally adding one vertex to its partial strategy following the state transition rule which favors the moves to more lightly-weighted vertices that are also connected by the edges with denser pheromone and less cost. For the $k$th ant at $v_i$, the next vertex $v_j$ to visit can be determined by the pseudo-random-proportional rule [21] so as to balance the discover of new edges and the utilization of cumulated knowledge. The desirability $\eta(i,u)$ of adding edge $(i,u)$ to the partial strategy is dynamically determined by the reverse of the cost associated with the edge $(i,u)$ and vertex $v_u$ as shown by

$$\eta(i,u) = \left\{ \left[ \frac{B(i,u)}{B^*(i,u)} \right] + \omega_1 \cdot \left[ \frac{N_0(u,t)}{N_0^*(u,t)} \right]^{\rho_1} \right\}^{-1} \tag{21}$$

where $B(i,u)$ is the susceptance of edge $(i,u)$ considering the installed reactive compensation devices, $B^*(i,u)$ is the minimal susceptance of all the connected edges without taking reactive devices into account, $N_0(u,t)$ is the weight of $v_u$, and $N_0^*(u,t)$ is the minimal weight of all the connected $v_u$. If $\eta(i,u)$ are not all positive, only the connected $v_u$ with negative $\eta(i,u)$ will be considered in the state transition process.

*Procedure 3: Diversity development*

For each strategy construction step, the pheromone is updated based on the local pheromone updating rule [21] to increase the diversity of solutions. Once all the ants have reached $v_t$, the pheromone trial will be updated by the global updating rule as shown in

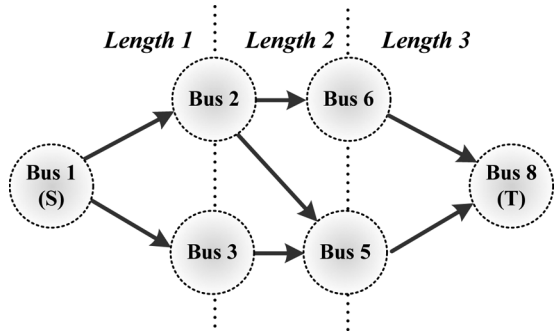


Fig. 5. Graph $G_g^3(V_g^3, E_g^3)$ composed of all the feasible paths containing three edges for the adjacency graph of Fig. 3(a).

$$\tilde{\tau}(i,j) \leftarrow (1-\rho) \cdot \tau(i,j) + \rho \cdot \Delta\tau_g(i,j) \tag{22}$$

where $\rho$ is a pheromone decay parameter with $0 < \rho < 1$ and $\Delta_g(i,j)$ is determined by

$$\Delta\tau_g(i,j) = \begin{cases} (F(\mathbf{R_0}) + H)^{-1}, & (i,j) \in E(\mathbf{R_0}) \\ \omega_1 \cdot \mu(i,j) \cdot (\hat{N}^*)^{-1}, & (i,j) \in \{E_g^e | e = m^* \, to \, L\} \\ 0, & \text{otherwise} \end{cases} \tag{23}$$

where $\mathbf{R}_0$ is the path of minimal cost $F(\mathbf{R})$, $H$ is the translation factor, and $\hat{N}^*$ is the minimal normalized number of switches considering all the feasible paths containing the edge $(i,j)$ in all the graphs $G_g^e(V_g^e, E_g^e)$ (for $e = m^*$ to $L$) derived by the path tracing algorithm as introduced in the following.

*Path tracing algorithm*

The path tracing algorithm is illustrated in Fig. 4, given the global parameters: $n$ (the total number of vertices), $s$ (the index of the starting vertex which represents the connecting transmission bus of BSU), $t^*$ (the index of the target vertex which represents the connecting transmission bus of target unit), and $\mathbf{A}$ (the adjacency matrix of the power system). Based on the property of adjacency matrix in Graph Theory, the paths containing $e$ edges can be traced from rear to front by recursively tracking the multiplication process to yield the power of matrix, $\mathbf{A}^e$. The traced paths can form a directed graph $G_g^e(V_g^e, E_g^e)$ with the ascending and descending layers between the two end vertices as depicted in Fig. 5.

In the path tracing computation module as seen in Fig. 1, the $m^{*\text{th}}$ to $L^{\text{th}}$ power of $\mathbf{A}$ are processed in parallel to trace the paths containing $m^*$ to $L$ edges, where $L$ is adjusted depending on the power system scale and the viable range of the number of switches in a black start path from the utility's point of view. The global pheromone updating rule, which is coalesced with the output of the path tracing computation module, can facilitate a compromise between the minimization of the number of switches and the exploration of the paths containing smaller susceptance and more compensation devices, while developing solution diversity.

*Procedure 4: Ranking adjustment*

The discovered candidates will be simulated automatically by PSS/E and EMTP in accordance with the user-specified energization mode. The simulated transient peak voltage and steady state voltage at each bus along the black start path will be used

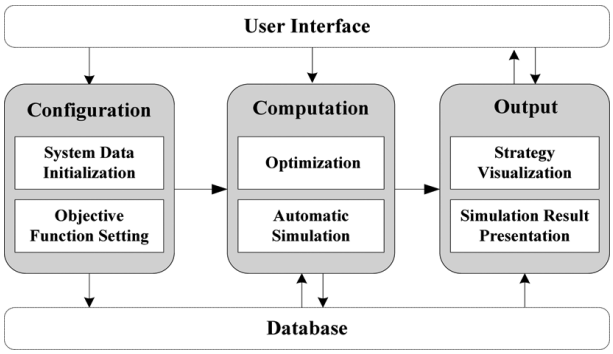


Fig. 6. Core modules of BSS.

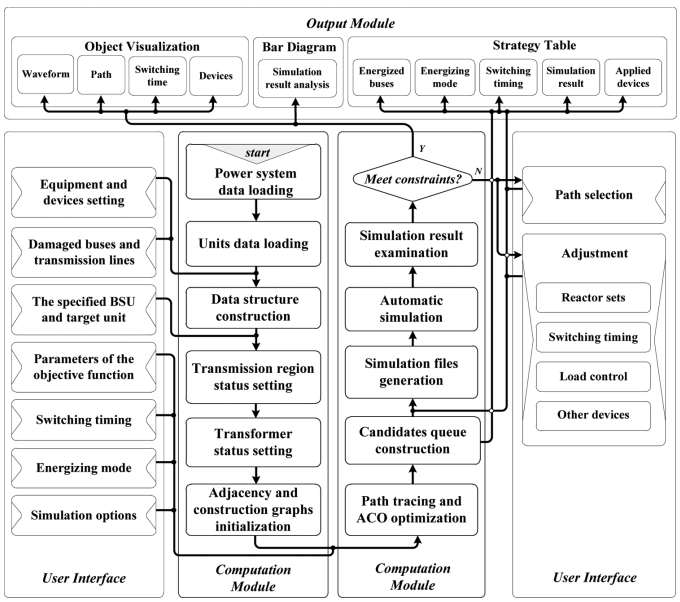


Fig. 7. Tasking and linking within and between the modules and user interface of BSS. (Note: The user interface block are the options of settings.)

to compute the corresponding $S(\mathbf{R})$ and the total $C_{\mathrm{p}}(\mathbf{R})$ for the adjustment in candidates' final ranking.

### B. Core Modules of BSS

The BSS is composed of configuration, computation, and output modules, as illustrated in Fig. 6. The tasking and linking of the core modules are presented in Fig. 7. Through the optimization computation, the BSS can display all the feasible black start strategies ranked by their corresponding priorities according to the latest system and equipment data, parameters of objective function, and other options of settings which are updated and tuned via the interactive GUI as seen in Fig. 8. For simulation automation, the strategies are written into files in a unified format and converted into a series of automation files to launch simulations in PSS/E 29 and ATP/EMTP 4. To offer intuitive and user-friendly demonstration of the output black start strategies and the corresponding simulation results, the components together with their energization mode, operation timing and simulated voltages on the energizing path are visualized by vivid icons, symbols, and charts with annotation in addition to table text and simulation waveform.

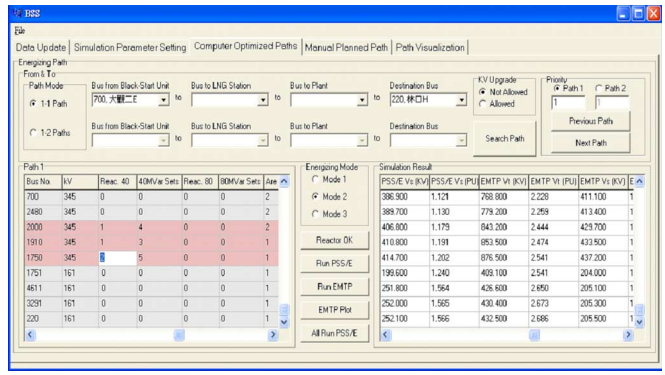


Fig. 8. GUI of BSS for the update of system and equipment data, configuration of optimization and simulation settings, and demonstration of strategies and simulation results.

TABLE I
SETTING OF WEIGHTS AND PENALTIES IN THE OBJECTIVE FUNCTION

| *Factors* | $\hat{B}$ | $\hat{N}$ | $\hat{T}$ | $\hat{V}_l$ | $\hat{V}_s$ |
|---|---|---|---|---|---|
| *Weight* | 1 | 1.5 | 10 | 1 | 1 |
| *Penalty* | 1 | 1.5 | 2 | 1 | 1 |

## IV. APPLICATION RESULT

Since the north region of TPS has intensive load but limited generation, TPC has manually planned the re-energizing paths for the north region, which start from the most powerful hydro BSUs in Region 2, i.e., *Ming-Tan* BSU and *Da-GuanII* BSU, to the target power plants in Region 1, i.e., *Xie-He* Plant and *Lin-Kou* Plant, in face of large-scale blackouts in Taiwan. Thus, the application cases, in which the BSS is used to compute the black start strategies from *Ming-Tan* and *Da-GuanII* to *Lin-Kou* and *Xie-He*, are demonstrated in this section to prove the effectiveness of BSS. The default weights and penalties in the objective function and the default energization modes for simulation are stated first. The application results of BSS are discussed in the sequel.

*Selection of weights and penalties*

BSS offers the flexibility that operators can input the desired values of weights and penalties through GUI to meet their particular planning needs. Based on TPC's elaborate calibration and tuning procedure, the default weights and penalties of the objective function are shown in Table I. The weight on the number of transformers is set much heavier than the other factors, i.e., $\omega_2 \gg \omega_1, \omega_3, \omega_4$, signifying that the value of $\hat{T}$ will be kept in its minimum as the re-energization of transmission system is required to be kept in the same voltage level as far as possible during black start. The weight on the number of switches is heavier than the number of susceptance because the switching operation would cause increasing risks resulted from transient phenomena and prolonged restoration duration. The penalties are set to 1 in general unless there is a need of the stressing force empowered by the exponent such as the case of TPC, where the penalty of $\hat{N}$ is set to 1.5 to prevent the number of switches from being excessively distant from its minimum.

*Energization modes*

Operators can also specify the desired energization mode of the output black start paths through GUI. There are three default energization modes [29], [31], given here.

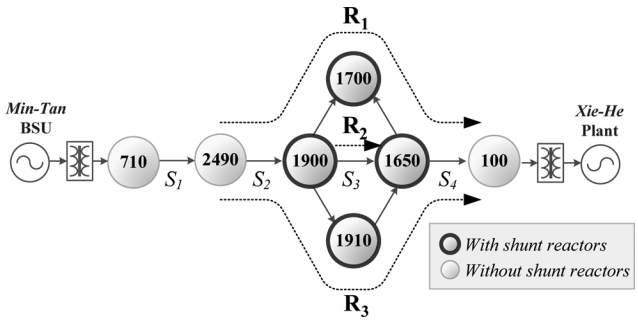


Fig. 9. Top three black start paths from *Min-Tan* BSU to *Xie-He* Plant.

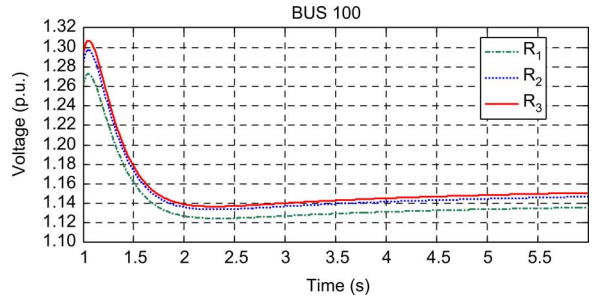


Fig. 10. Simulated voltage variations at Bus 100 of the top three black start paths during black start procedure under Mode 2 (linked to PSS/E).

1) Mode 1: Sequentially energize each transmission line of $\mathbf{R}$ with full voltage of BSU;
2) Mode 2: Simultaneously energize all the transmission lines of $\mathbf{R}$ with full voltage of BSU;
3) Mode 3: Simultaneously energize all the transmission lines of $\mathbf{R}$ with step-rising voltage of BSU.

### A. Test of BSS's Applicability

By the BSS's computation, the optimal black start paths under the three default energizing modes from *Ming-Tan* BSU to *Xie-He* Plant all turned out to be the path $\mathbf{R_1}$, as illustrated in Fig. 9, which is correspondent with one of the plans established by TPC for the northern Taiwan [29], [31]. In addition to the strategy of first priority, for comprehensive views, BSS also displays all the other feasible strategies ranked by their respective priorities; in this case, $\mathbf{R_2}$ and $\mathbf{R_3}$ are evaluated as the strategies of second and third priorities, respectively. As the terminal buses are preset by TPC, the strategy's priority is determined based on its cost value defined by (12). The less cost the strategy has, the higher priority it will receive. Table II is the report of every cost factor's value of $\mathbf{R_1}$, $\mathbf{R_2}$, and $\mathbf{R_3}$ that composes $C_{\mathrm{p}}(\mathbf{R}_i)$. It is shown that the $\hat{N}$ factor of $\mathbf{R}_1$ is the largest among the three strategies, possessing one switch in excess of the minimum; yet the $\hat{B}$ factor of $\mathbf{R}_1$ is the smallest since it explores more shunt reactors of larger capacity. For the observation of transient phenomena, BSS also provides the simulated voltage variation and three-phase waveform at each bus on the energizing path. Fig. 10 demonstrates the simulated voltage variations under Mode 2 at the terminal transmission bus connected to *Xie-He* Plant of the top three strategies. It is shown that $\mathbf{R}_1$ has the lowest transient and steady state voltage comparing to the others. As the voltage along the energizing path would keep rising progressively under Mode 2, the simulation result at the terminal bus on the path reveals that $\mathbf{R}_1$ is the most secure solution in terms of the transient and overvoltage risk. By applying proper sets of the installed 40-MVar three-phase shunt reactors connected to Bus 1900, Bus 1700 and Bus 1650, it is proven that the voltage variations at each bus on $\mathbf{R}_1$, $\mathbf{R}_2$, and $\mathbf{R}_3$ can be regulated within the secure range [30] during the black start procedure; the three strategies are thus justified to be feasible and applicable [29]. Further tests have also proven that the strategies generated via BSS is corresponding to the other black start plans established by TPC from the BSUs to the designated target units [29], while with all the feasible backup plans included.

TABLE II
VALUES OF THE NORMALIZED FACTORS FOR COST COMPUTATION

| Cost factors \ Strategy | | 1st Priority $\mathbf{R}_1$ | 2nd Priority $\mathbf{R}_2$ | 3rd Priority $\mathbf{R}_3$ |
|---|---|---|---|---|
| $\hat{B}$ | | -2.098 | -2.034 | -1.165 |
| $\hat{N}$ | | 1.250 | 1.250 | 1.000 |
| $\hat{T}$ | | 1.000 | 1.000 | 1.000 |
| $\hat{V}_t$ | *Mode 1* | 1.143 | 1.162 | 1.165 |
| | *Mode 2* | 1.255 | 1.276 | 1.282 |
| | *Mode 3* | 1.094 | 1.102 | 1.103 |
| $\hat{V}_s$ | *Mode 1* | 1.125 | 1.133 | 1.134 |
| | *Mode 2* | 1.120 | 1.128 | 1.129 |
| | *Mode 3* | 1.091 | 1.099 | 1.100 |
| *Total* $C_{\mathrm{p}}(\mathbf{R}_i)$ | *Mode 1* | 12.266 | 12.357 | 12.634 |
| | *Mode 2* | 12.373 | 12.466 | 12.746 |
| | *Mode 3* | 12.183 | 12.263 | 12.538 |

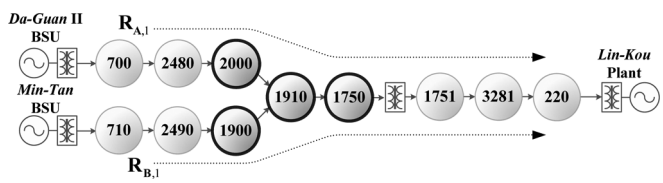


Fig. 11. Optimal black start paths from *Da-GuanII* BSU and *Min-Tan* BSU to *Lin-Kou* Plant, respectively.

### B. Test of BSS's Adaptability

As seen in Fig. 11, the optimal black start paths from *Ming-Tan* BSU and *Da-GuanII* BSU to *Lin-Kou* Plant provided by BSS are $\mathbf{R}_{\mathrm{A},1}$ and $\mathbf{R}_{\mathrm{B},1}$, respectively, where the subscript number $n$ separated by the comma denotes the $n$th priority. It is confirmed that $\mathbf{R}_{\mathrm{A},1}$ and $\mathbf{R}_{\mathrm{B},1}$ correspond to the rest black start plans established by TPC for the north region [29], [31]. Suppose that the transmission line between Bus 3281 and Bus 220 is damaged during the blackout; the pre-established plans must therefore be updated accordingly in a timely fashion. In response to the system change, BSS can rapidly generate the alternative set of optimal strategies and the respective simulation results. To re-energize lines from *Da-GuanII* BSU to *Lin-Kou* Plant, the original path $\mathbf{R}_{\mathrm{A},1}$ is replaced by $\mathbf{R}'_{\mathrm{A},1}$ as seen in Fig. 12. As Bus 1751 is on one side connected to a transformer and on the other connected to the underground cables with large phase-to-ground capacitance, the voltage variation at Bus 1751 requires careful observation for the path's feasibility confirmation. Fig. 13 shows the simulated voltage at Bus 1751 while energizing lines following $\mathbf{R}'_{\mathrm{A},1}$ under Mode 2. The red solid line and the blue dotted line denote the voltage variations before and after applying the proper sets

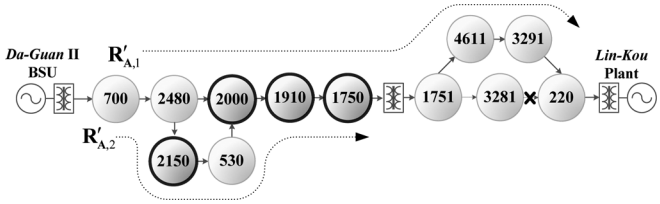


Fig. 12. Top two alternative black start paths from *Da-GuanII* BSU to *Lin-Kou* Plant after the transmission line from Bus 3281 to Bus 220 is damaged.

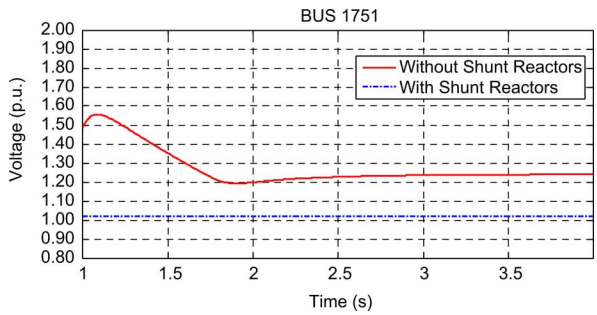


Fig. 13. Voltage variations of Bus 1751 before and after applying the shunt reactors at Bus 2000, 1910, and 1750 while energizing transmission lines along $\mathbf{R}'_{A,1}$ under Mode 2 (linked to PSS/E).

TABLE III
APPLIED SETS OF 40-MVAR SHUNT REACTOR FOR THE BLACK START STRATEGIES $\mathbf{R}'_{A,1}$ AND $\mathbf{R}'_{A,2}$

| *Location* | *Available sets of reactors* | *Applied sets of reactors* |
|---|---|---|
| *BUS 2000* | 4 | 1 |
| *BUS 1910* | 3 | 2 |
| *BUS 1750* | 5 | 2 |

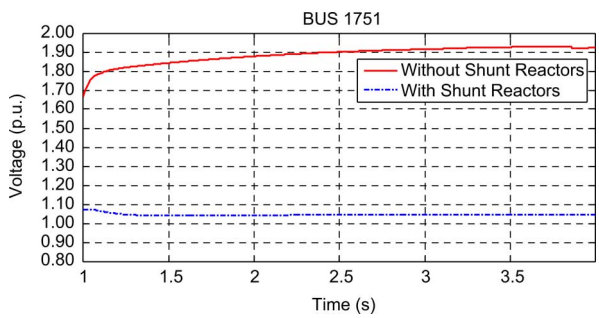


Fig. 14. Voltage variations of Bus 1751 before and after applying the shunt reactors at Bus 2000, 1910, and 1750 while energizing transmission lines along $\mathbf{R}'_{A,2}$ under Mode 2 (linked to PSS/E).

of 40-MVar shunt reactors at Bus 2000, 1910, and 1750 as noted in Table III, respectively. It reveals that after applying the reactors, the transient voltage at Bus 1751 can be lowered down to 1.020 p.u., which is within the secure range.

The alternative strategy with second priority, i.e., $\mathbf{R}'_{A,2}$, is also demonstrated in Fig. 12. The corresponding simulation result of $\mathbf{R}'_{A,2}$ under the same simulation settings as $\mathbf{R}'_{A,1}$ is presented in Fig. 14. It is clearly shown that the overvoltage phenomenon at Bus 1751 is severe while adopting the strategy $\mathbf{R}'_{A,2}$, which further justify the higher priority of $\mathbf{R}'_{A,1}$ because $\mathbf{R}'_{A,1}$ has fewer switches, less susceptance, and more secure transient and steady-state voltage behavior. However, as $\mathbf{R}'_{A,2}$ explores more buses that are connected to reactive devices of larger capacity, e.g., Bus 2150, which connects to five sets of 40-MVar shunt reactors, the strategy $\mathbf{R}'_{A,2}$ is also considered as a feasible alternative countermeasure [29]. The application result not only justifies the adaptability of BSS while encountering changes in power systems, but also demonstrates the flexibility of BSS in simulation scenario settings for ease of strategy verification and validation.

## V. CONCLUSION

For isolated power systems such as TPS, a reliable and efficient black start procedure is more important than interconnected power systems. In this paper, a black start decision-supporting system (BSS) has been developed. The BSS currently serves as an offline black start planning tool in TPC with high computation efficiency. Built from the modular structure, the supporting functions of BSS can be easily extended and further integrated into online monitoring and control systems. BSS significantly reduces the evaluation and simulation time of black start strategies and offers reliable solutions as references, which the dispatchers can make proper adjustments according to the prevailing operation concerns, such that the pressure of dispatchers can be greatly relieved while dealing with a severe blackout.

## ACKNOWLEDGMENT

The authors greatly appreciate the support and cooperation of the Department of System Operations, Taiwan Power Company.

## REFERENCES

[1] "US-Canada Power Outage Task Force. Final report on the blackout in the United States and Canada," Aug. 2003 [Online]. Available: http://www.ferc.gov [EB/OL]
[2] "Defense meteorological satellite program. Japan earthquake and tsunami," Nat. Geophysical Data Center, Mar. 19, 2011. [Online]. Available: http://earthobservatory.nasa.gov [EB/OL]
[3] "Investigation Report of 729 Event of Taiwan Power Company, Department of Economic Affairs (in Chinese)," Taiwan Power Company, 1999.
[4] L. L. Tsai, "Struggling in power dispatching during the devastating 921 earthquake in Taiwan," *Monthly J. of Taipower's Eng., (in Chinese)*, vol. 618, pp. 54–66, Feb. 2000.
[5] M. M. Adibi and D. Scheurer, "System operations challenges-Issues and problems in power system restoration," *IEEE Trans. Power Syst.*, vol. 3, no. 1, pp. 123–126, Feb. 1988.
[6] M. M. Adibi and L. H. Fink, "Special considerations in power system restoration," *IEEE Trans. Power Syst.*, vol. 7, no. 4, pp. 1419–1427, 1992.
[7] M. M. Adibi, R. W. Alexander, and B. Avramovic, "Overvoltage control during restoration," *IEEE Trans. Power Syst.*, vol. 7, no. 4, pp. 1464–1470, 1992.
[8] P. G. Boliaris, J. M. Prousalidis, N. D. Hatziargyriou, and B. C. Papadias, "Simulation of long transmission lines energization for black start studies," in *Proc. Mediterranean Electrotech. Conf.*, 1994, vol. 3, pp. 1093–1096.
[9] M. M. Adibi and L. H. Fink, "Power system restoration planning," *IEEE Trans. Power Syst.*, vol. 9, no. 1, pp. 869–875, Feb. 1994.
[10] F. P. de Mello and J. C. Westcott, "Steam plant startup and control in system restoration," *IEEE Trans. Power Syst.*, vol. 9, no. 1, pp. 93–101, Feb. 1994.
[11] M. M. Adibi *et al.*, "Power system restoration-The second task force report," *IEEE Trans. Power Syst.*, vol. 2, no. 4, pp. 927–933, Nov. 1987.
[12] M. M. Adibi *et al.*, "Power system restoration-A task force report," *IEEE Trans. Power Syst.*, vol. 2, no. 2, pp. 271–277, May 1987.

[13] *System Restoration From Black Start Resources, NERC*, Standard EOP-005-2, Mar. 2011.

[14] *"Operation Handbook: Policy 5, Emergency Procedures,"* UCTE, 2006.

[15] "Nodal Operating Guides Section 8, Attachment E: Detailed Black Start Information," ERCOT, 2011.

[16] T. Sakaguchi and K. Matsumoto, "Development of a knowledge based system for power system restoration," *IEEE Trans. Power Syst.*, vol. PS-102, no. 2, pp. 320–329, Apr. 1983.

[17] D. S. Kirschen and T. L. Volkmann, "Guiding a power system restoration with an expert system," *IEEE Trans. Power Syst.*, vol. 6, no. 2, pp. 558–565, Apr. 1991.

[18] M. M. Adibi, R. J. Kafka, and D. P. Milanicz, "Expert system requirements for power system restoration," *IEEE Trans. Power Syst.*, vol. 9, no. 3, pp. 1592–1598, Jun. 1994.

[19] C. Wang and Y. Liu, "Group intelligent decision support system for power system skeleton restoration," in *Proc. 20th IEEE Int. Conf. Tools Artif. Intell.*, 2008, pp. 126–129.

[20] Y. Hou, C. C. Liu, K. Sun, P. Zheng, S. Liu, and D. Mizumura, "Computation of milestones for decision support during system restoration," *IEEE Trans. Power Syst.*, vol. 26, no. 3, pp. 1399–1409, Jun. 2011.

[21] K. Y. Lee and M. A. El-Sharkawi, *Modern Heuristic Optimization Techniques: Theory and Applications to Power Systems*. New York: IEEE Press/Wiley-Interscience, 2008, pp. 96–96.

[22] G. Lambet-Torres, H. G. Martins, M. P. Coutinho, C. P. Salomon, and L. S. Filgueiras, "Particle swarm optimization applied to restoration of electrical energy distribution systems," in *Proc. Int. Symp. Intell. Computation Applicat.*, 2008, pp. 228–238.

[23] G. Lambert-Torres, H. G. Martins, M. P. Coutinho, L. E. B. Silva, F. M. Matsunaga, R. A. Carminati, and J. N. Cabral, "Genetic algorithm to system restoration," in *Proc. World Congress on Electron. Elect. Eng.*, 2009, vol. 3, pp. 9–14.

[24] W. J. Liu, Z. Z. Lin, F. S. Wen, and G. Ledwich, "Intuitionistic fuzzy Choquet integral operator-based approach for black start decision-making," *IET Gen., Transm. Distrib.*, vol. 6, no. 5, pp. 378–386, 2012.

[25] J. L. Yu, J. B. Yang, and S. H. Zheng, "A novel method for ranking black start plans based on data envelopment analysis," in *Proc. Power Energy Eng. Conf.*, 2012, pp. 1–4.

[26] S. Zeng, Z. Lin, F. Wen, and G. Ledwich, "A new approach for power system black start decision-making with vague set theory," *Int. J. Elect. Power Energy Syst.*, vol. 34, no. 1, pp. 114–120, 2012.

[27] W. Sun, C. C. Liu, and L. Zhang, "Optimal generator start-up strategy for bulk power system restoration," *IEEE Trans. Power Syst.*, vol. 26, no. 3, pp. 1357–1366, Jun. 2011.

[28] N. Saraf, K. McIntyre, J. Dumas, and S. Santoso, "The annual black start service selection analysis of ercot grid," *IEEE Trans. Power Syst.*, vol. 24, no. 4, pp. 1867–1874, Aug. 2009.

[29] "Report of Assessment on Black Start Capacity," Dept. Syst. Operations, Taiwan Power System, 2008.

[30] "System Operation Criteria for Taiwan Power System," Taiwan Power Company, 2012.

[31] "Report of Planning of Transmission Line Energizing Route During Black Start," Dept. Syst. Operations, Taiwan Power Co., 2006.

[32] *Power System Restoration: Methodologies and Implementation Strategies*, M. M. Adibi, Ed. New York: Wiley/IEEE Press, 2000.

[33] H. Kuisti, "Energization of an unloaded transmission grid as part of restoration process," in *Proc. Int. Conf. Power Syst. Transients*, 2003. [Online]. Available: www.ipst.org/TechPapers/2003/IPST03Paper4b-1.pdf

[34] L. Kocis, "Ferroresonances during black starts—criterion for feasibility of scenarios," in *Proc. Int. Conf. Power Syst. Transients*, 2007. [Online]. Available: www.ipst.org/techpapers/2007/ipst_2007/papers_IPST2007/Session8/168.pdf

[35] "Transmission system planning criteria for taiwan power system," Taiwan Power Co., 2008.

[36] M. Dorigo and L. M. Gambardella, "Ant colony system: A cooperative learning approach to the traveling salesman problem," *IEEE Trans. Evol. Comput.*, vol. 1, no. 1, pp. 53–66, Jan. 1997.


**Yi-Ting Chou** was born in Taipei, Taiwan, in 1983. She received the B.S. degree from National Cheng Kung University, Tainan, Taiwan, in 2006, and the M.S. and Ph.D. degrees at National Taiwan University, Taipei, Taiwan, in 2008 and 2012, respectively, all in electrical engineering.

She is currently a Postdoctoral Research Fellow with the Graduate Institute of Electrical Engineering, National Taiwan University, Taipei, Taiwan. Her main research interests include power system optimization, protection, and stability monitoring and control.

**Chih-Wen Liu** (F'13) was born in Taiwan in 1964. He received the B.S. degree from National Taiwan University, Taipei, Taiwan, and the M.S. and Ph.D. degrees from Cornell University, Ithaca, NY, USA, in 1987, 1992, and 1994, respectively, all in electrical engineering.

Since 1994, he has been with National Taiwan University, Taipei, Taiwan, where he is a Professor of electrical engineering. His main research interests include application of computer technology to power system monitoring, protection, and control. His other research interests include motor control and power electronics.

**Yi-Jen Wang** was born in Taiwan in 1961. He received the B.S. degree from National Taiwan University of Science and Technology, Taipei, Taiwan, in 1986, and the M.S. and Ph.D. degrees from National Taiwan University, Taipei, Taiwan, in 1990 and 2007, respectively, all in electrical engineering.

Since 1990, he has been with Tungnan University, Taipei, Taiwan, where he is an Associate Professor of electrical engineering. His research interests include power system analysis and application of synchronized phasor measurements to enhance power system transient stability.

**Chin-Chung Wu** was born in Taipei, Taiwan, in 1964. He received the B.S.E.E. and M.S.E.E. degrees from National Taiwan Institute of Technology, Taipei, Taiwan, in 1990 and 1993, respectively, and the Ph.D. degree from National Taiwan University of Science and Technology, Taipei, Taiwan, in 2003, all in electrical engineering.

Dr. Wu is currently the Chief of the Planning Division of the Department of System Operations. His research interests are in power system operation and analysis, particularly in system securities and dispatch control.

**Chao-Chi Lin** was born in Taipei, Taiwan, on August 28, 1972. He received the B.S.E.E. degree from National Taipei Institute of Technology, Taipei, Taiwan, in 1997, and the M.S.E.E. degree from the National Taiwan University of Science and Technology, Taipei, Taiwan, in 2007.

Currently, he is the Shift Leader of the Center Dispatching Control Center, Taiwan Power Company. His interests include power system operations and regulations, power system protective relaying, and blackout regulations analysis and planning.